Supported in part by DOE Grant # DE-SC0023491

Production of J/ψ vs Multiplicity

In $\sqrt{s}$ = 510 GeV p+p Collisions with STAR at RHIC

Brennan Schaefer (Lehigh University)
for the STAR Collaboration 24.09.24

Motivation for J/ψ studies

J/ψ was long seen as a golden probe for the presence of the QGP

Suppression of J/ψ is seen more in central than peripheral A+A collisions

Also suppressed in high compared to low multiplicity p+p?

as seen in Wei Zhang's talk tomorrow

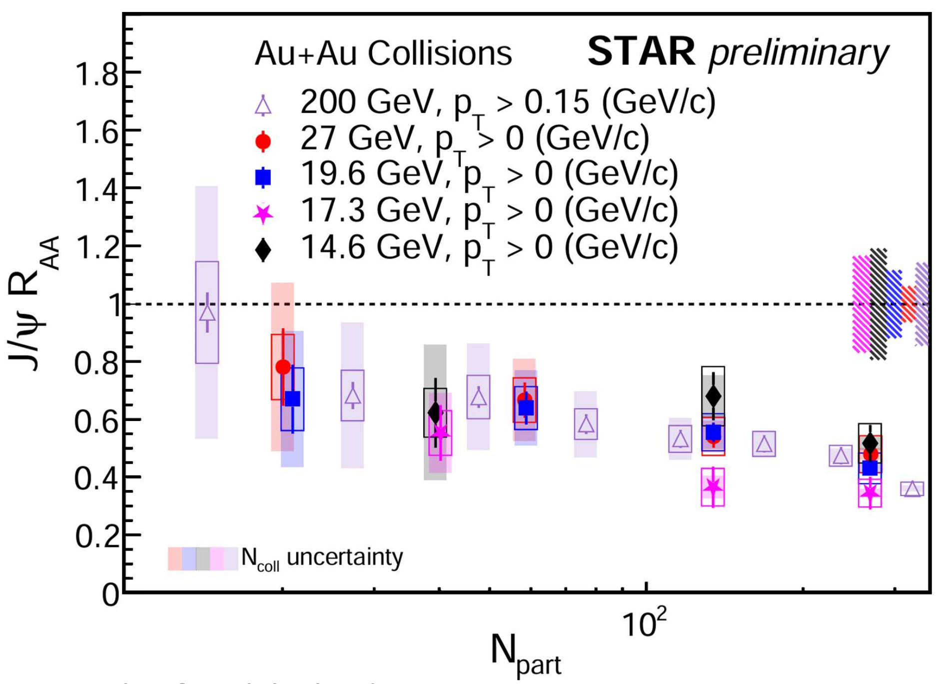

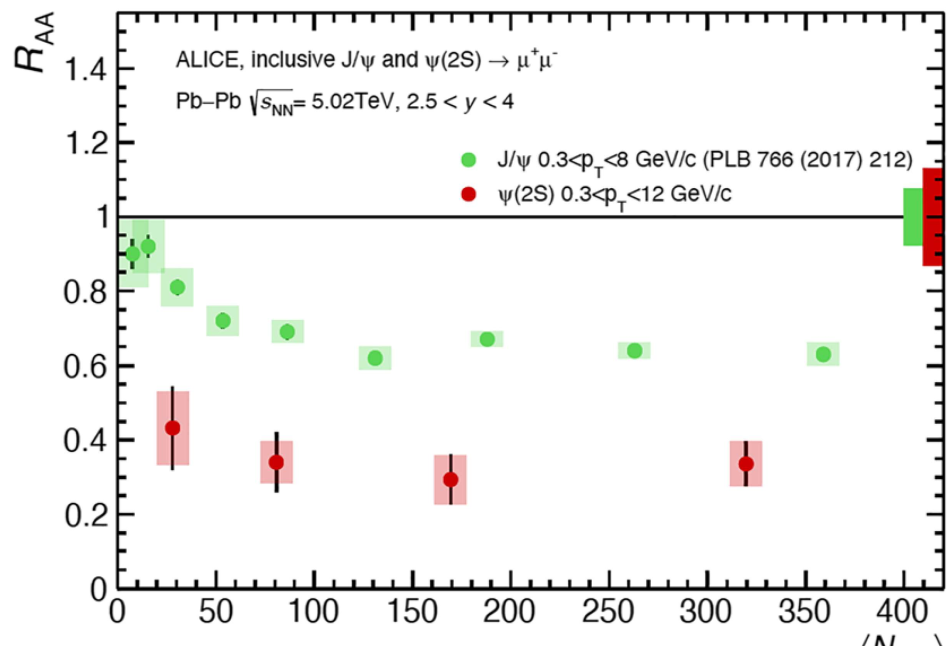

ALICE, Phys. Rev. Lett. 132 (2024) 042301

Hard Scattering Processes within NRQCD

$$d\sigma \sim f(x_1) \otimes f(x_2) \otimes \hat{\sigma}^{x_1+x_2\to[c\bar{c}]+X} \otimes H^{[c\bar{c}]\to J/\psi}$$

color−singlet model

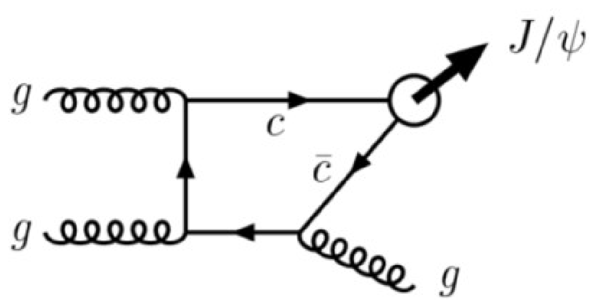

M. Kramer hep-ph/0106120

color−octet model

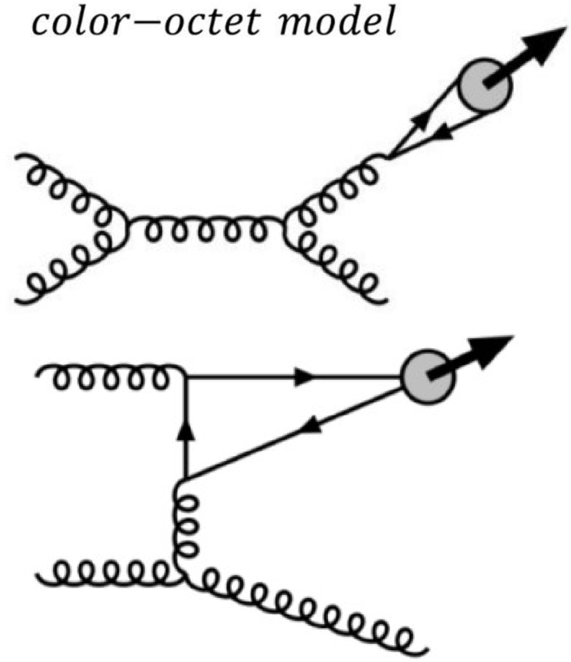

A production baseline

Predictions from NRQCD as implemented in Pythia 6, purposefully involving only hard scattering, and neglecting parton clusters with multi-parton interactions. Even beauty hadron feeddown is absent.

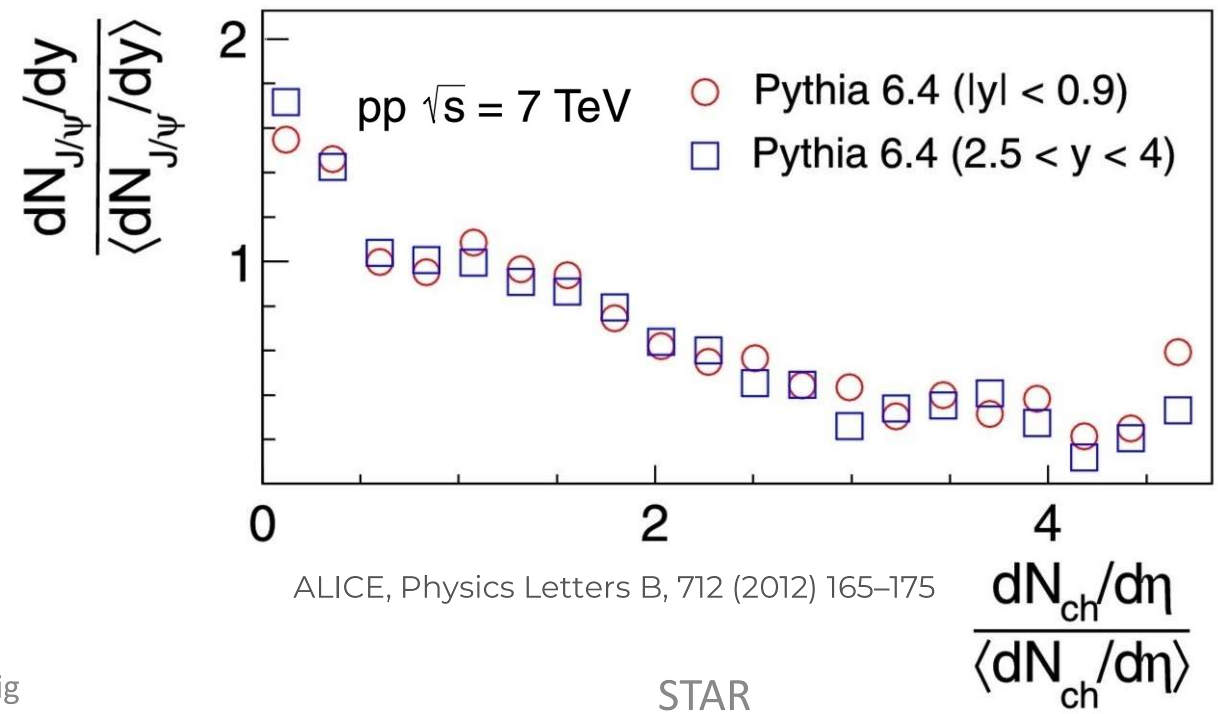

ALICE, Physics Letters B, 712 (2012) 165–175

Earlier Measurements

At multiple energies, J/ψ production has been found to rise with respect to event multiplicity, at rates that are faster than linear.

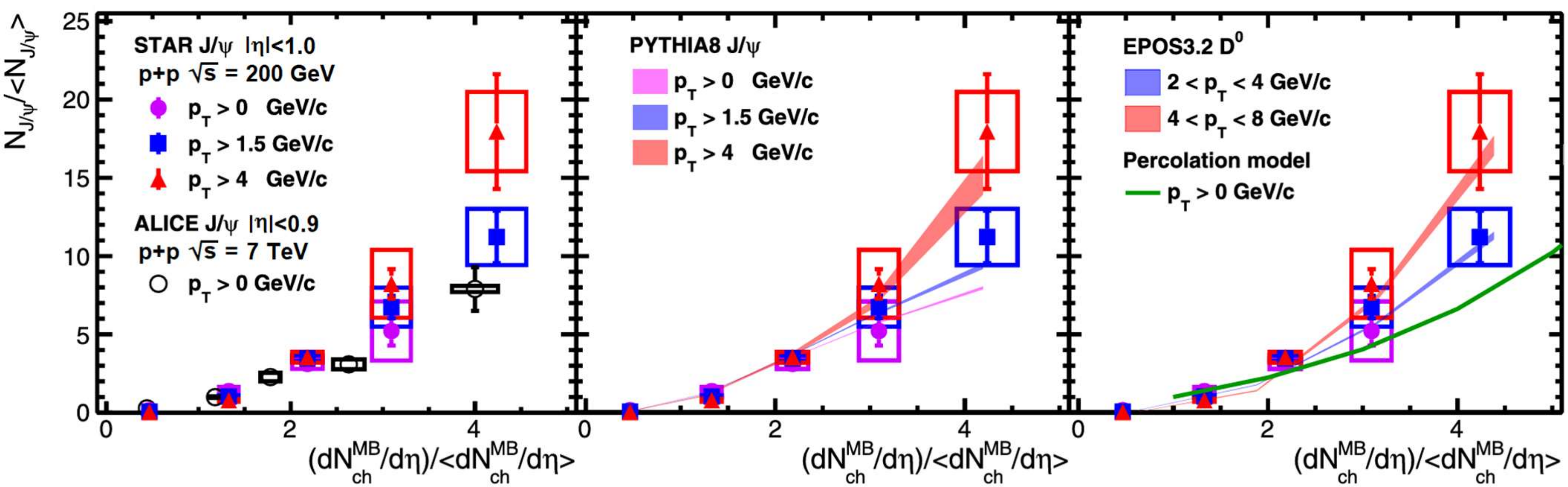

STAR, Physics Letters B 786 (2018) 87–93

Multi-Parton Interactions

Events that feature more numerous multi-parton interactions are more likely to feature small impact parameters of opposing partons, resulting in enhanced hard scattering processes such as J/ψ production

S. Weber et al. Eur. Phys. J. C (2019) 79:36

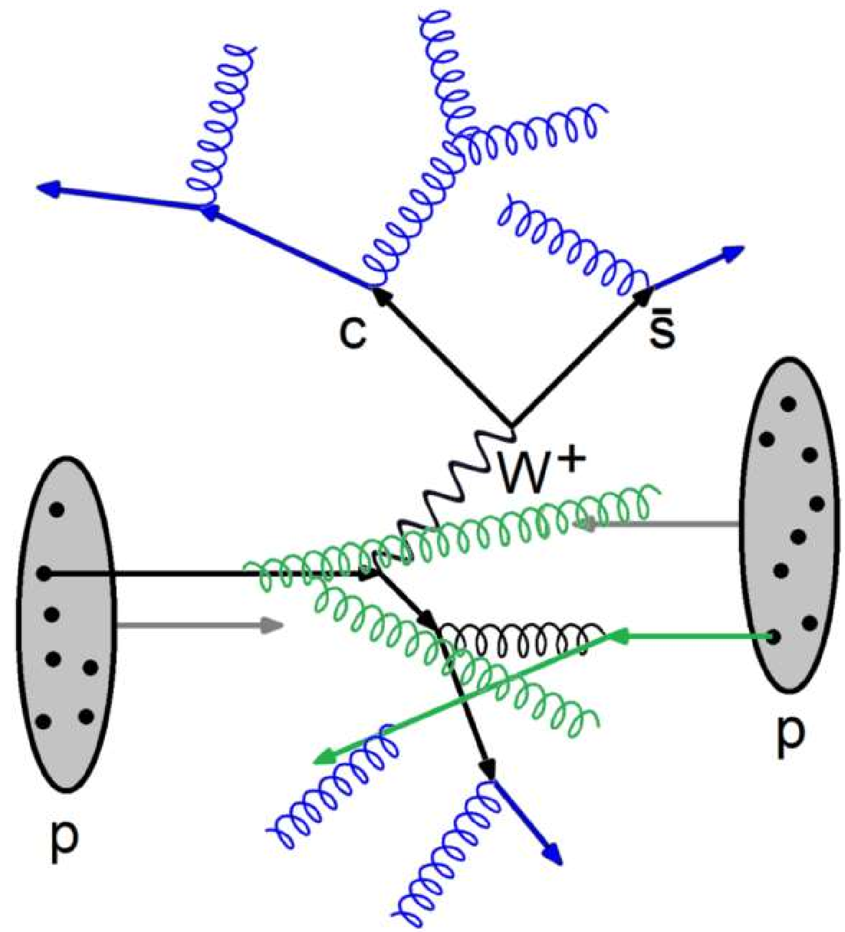

Percolation

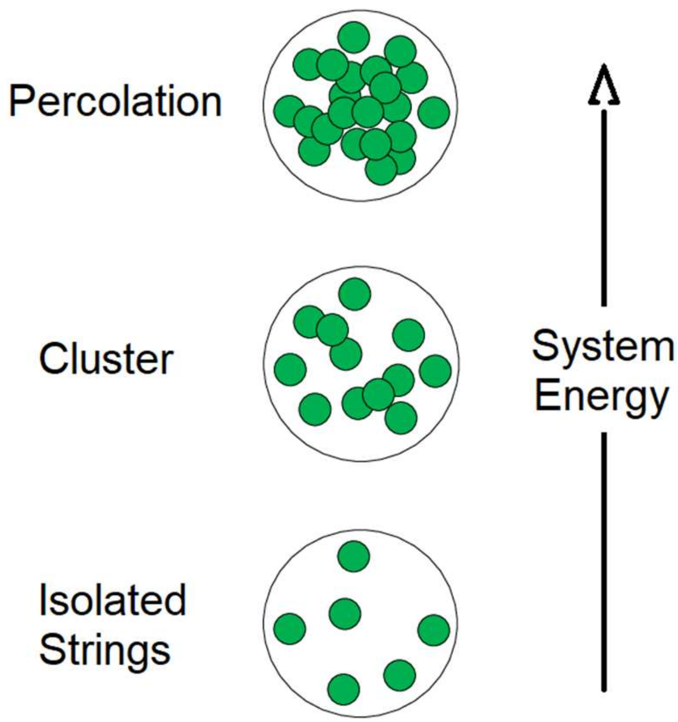

Percolation of color strings may similarly contribute to the faster than linear increase by diminishing soft hadron production in relation to J/ψ production

E. G. Ferreiro, C. Pajares, Phys.Rev.C 86 (2012) 034903

The STAR Detector

Barrel Electromagnetic Calorimeter
- 0.05 x 0.05 (phi x eta) towers
- $|\eta|<1.0$

Time of Flight
- r=208cm, Δt=100ps, $|\eta|< 0.9$

Beam-Beam Counter
- $3.8 < |\eta| < 5.1$

Time Projection Chamber
- 52.8 m^3, $|\eta|< 1.0$

Vertex Position Detector
- $4.24 < |\eta| < 5.1$

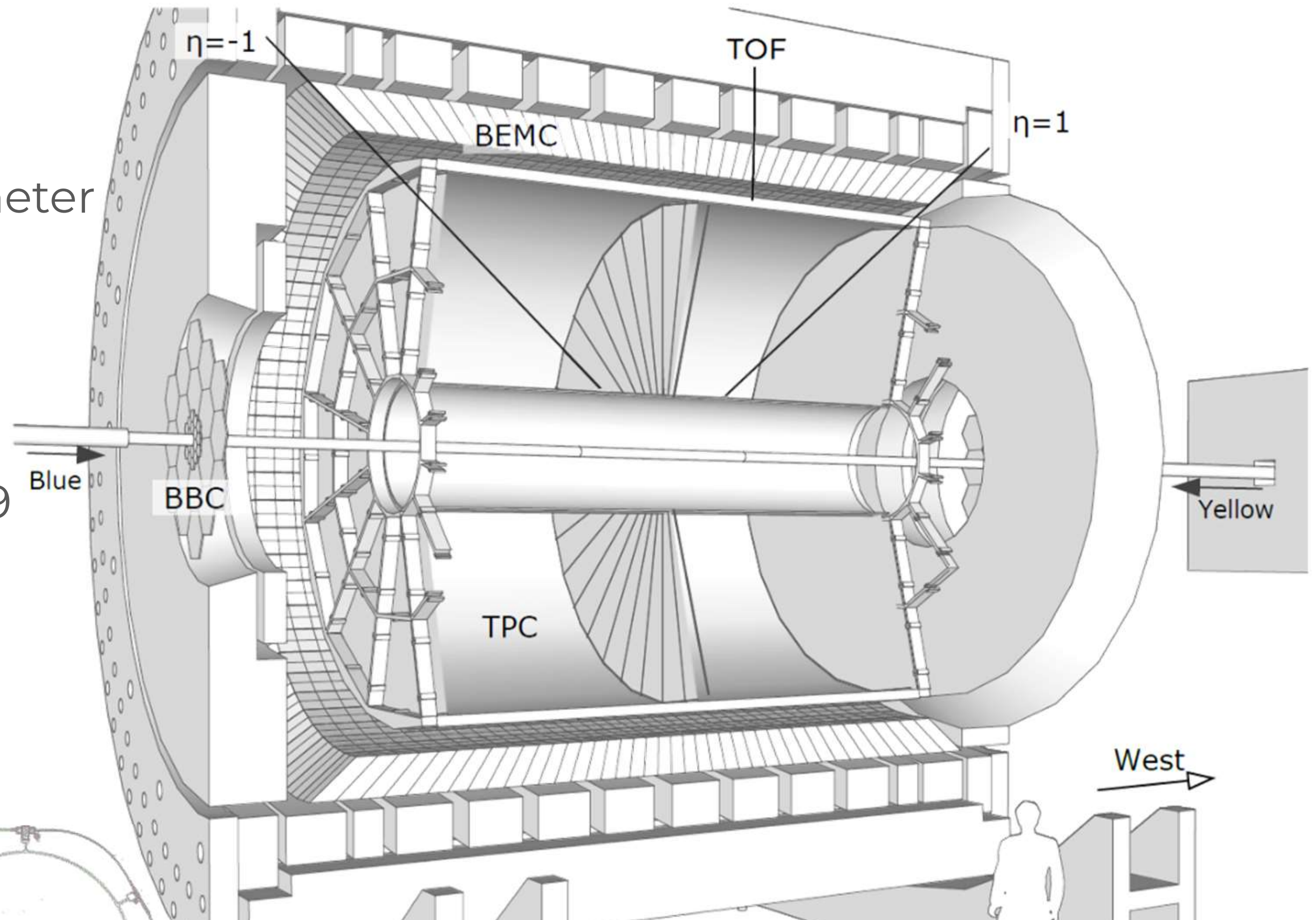

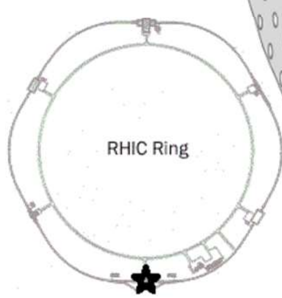

STAR

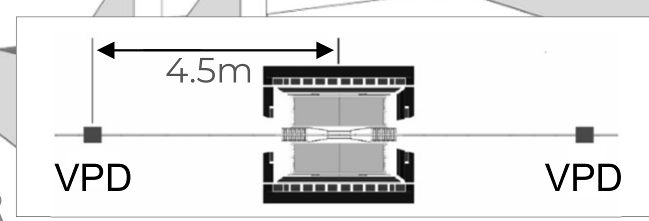

Detector Usage

(VPD) Vertex Position Detector
    Measure vertex z-position

(BEMC) Barrel EM Calorimeter
    Trigger on, identify electrons

(BBC) Beam-Beam Counter
    Min-bias trigger

(TPC) Time Projection Chamber
    Tracking and dE/dx

(TOF) Time of Flight
    Pileup track rejection
    Multiplicity estimation
    Slow non $e^{\pm}$ veto

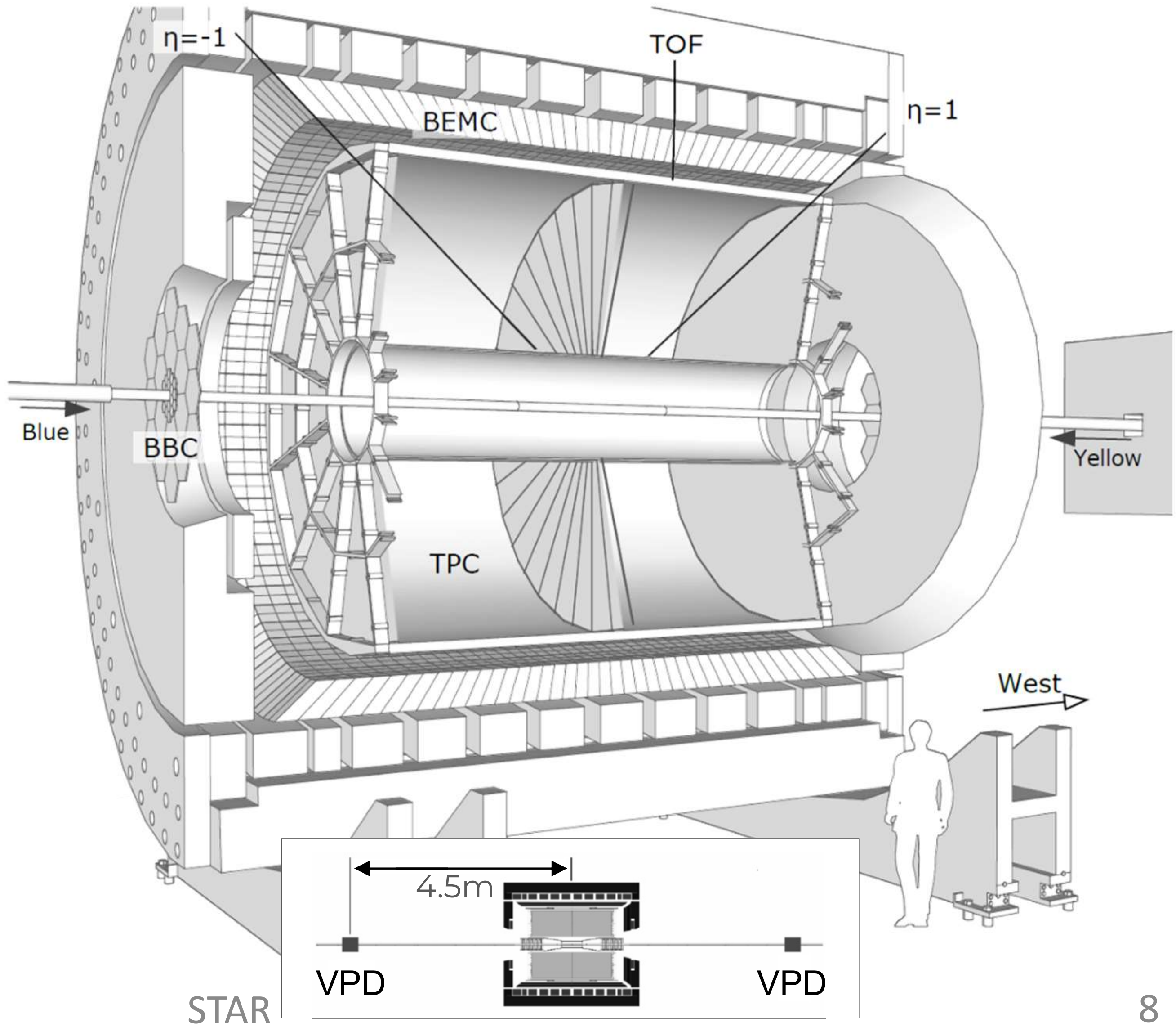

STAR

Dataset

2017 STAR *p+p* at $\sqrt{s}$ = 510 GeV (79.5 pb^{-1})

4x increase in luminosity above J/ψ vs mult. in *p+p* 200 GeV result

Event Selection

Trigger: BEMC Tower with E > 4.2 GeV

Events in ±40cm from z = 0

Vertex quality selections

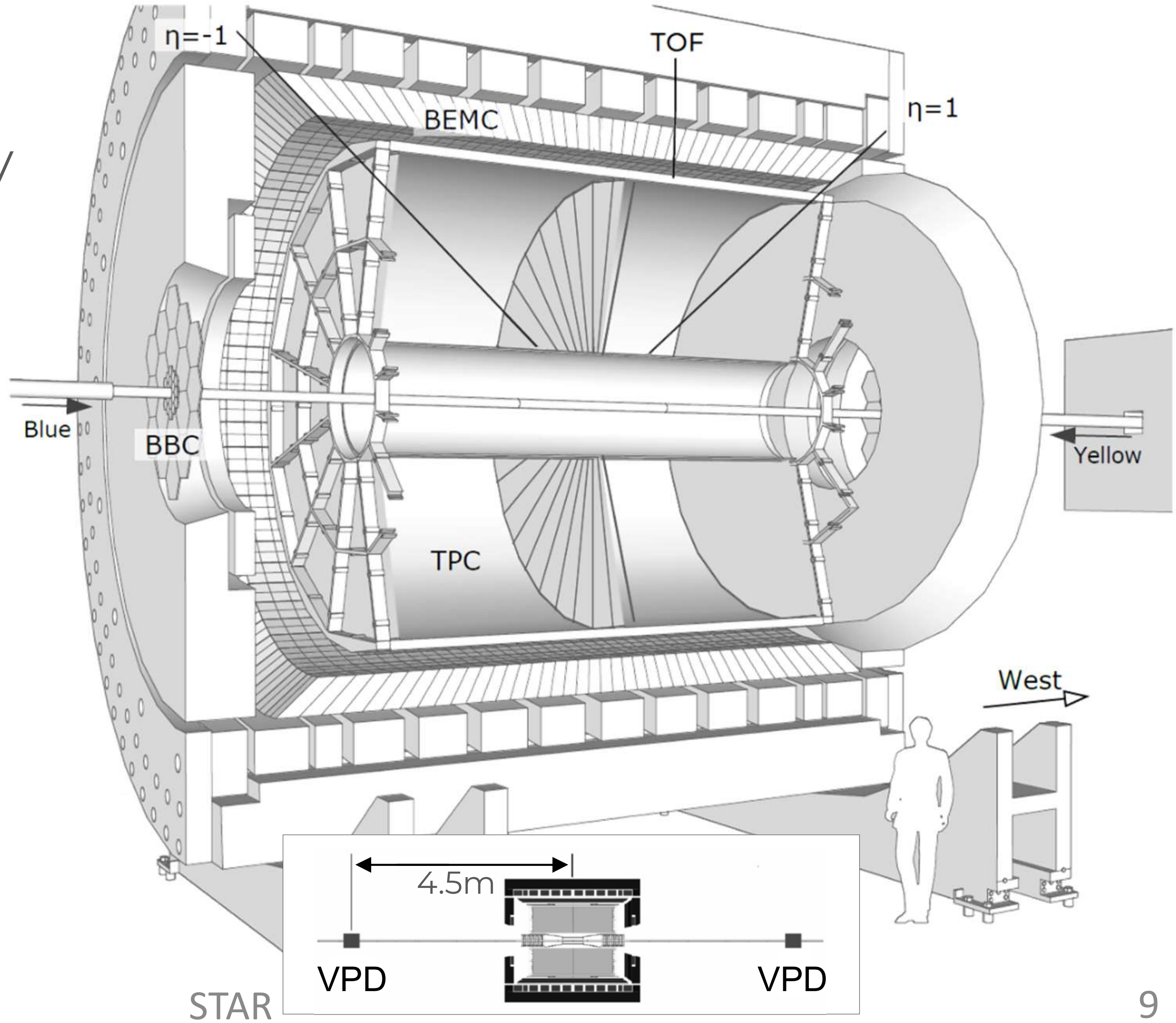

STAR

Event Multiplicity

Event activity is characterized using TOF multiplicity: number of tracks matched to TOF hits

TOF Mult. Track Selection

Track Quality Selections

DCA to PV < 1.5 cm

$|\eta|<1.0$

Track Matched to TOF Hit

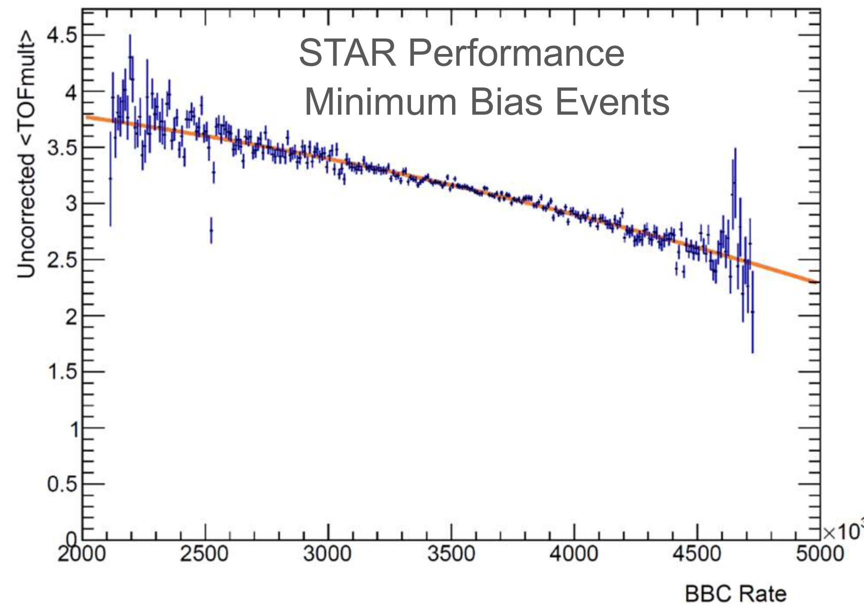

Correction for dependence of tracking efficiencies on occupancy effects accompanying luminosity rate

Correction for trigger efficiencies found from simulation

Decay Product Selection

Track Selection

$p_T > 0.2$ GeV/c

$|\eta|<1.0$

DCA to PV < 1.5 cm

Track Quality Selections

Trigger $e^{\pm}$ Selection

Trigger: $E_{tower} > 4.2$ GeV

dE/dx: $-1.9 < n\sigma_e < 3.0$

BEMC: $2/3 < E_{cluster}/p < 10/3$*

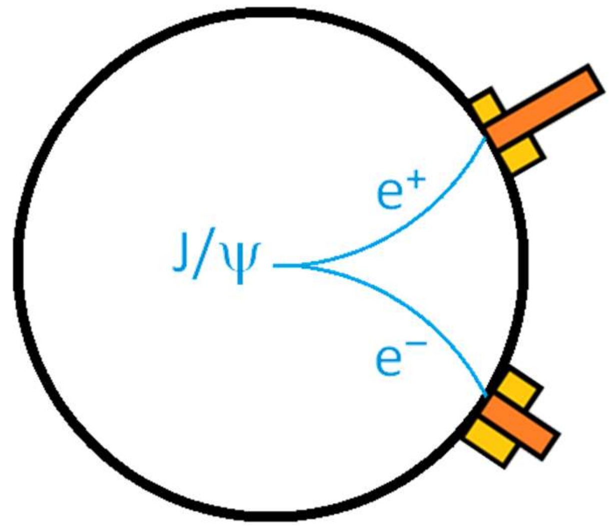

Associate $e^{\pm}$ Selection

Slow non $e^{\pm}$ veto ($0.97 < \beta < 1.03$)

OR

BEMC: $2/3 < E_{cluster}/p < 10/3$*

*BEMC Clusters: 3 towers

Analysis Procedure

Reconstruct J/ψ in the dielectron channel, using the invariant mass method

Construct unlike-sign invariant mass distribution

Fit distribution with CrystalBall peak + cubic polynomial for background

Centroid of CrystalBall core fixed to PDG world average

Width is variable in fit

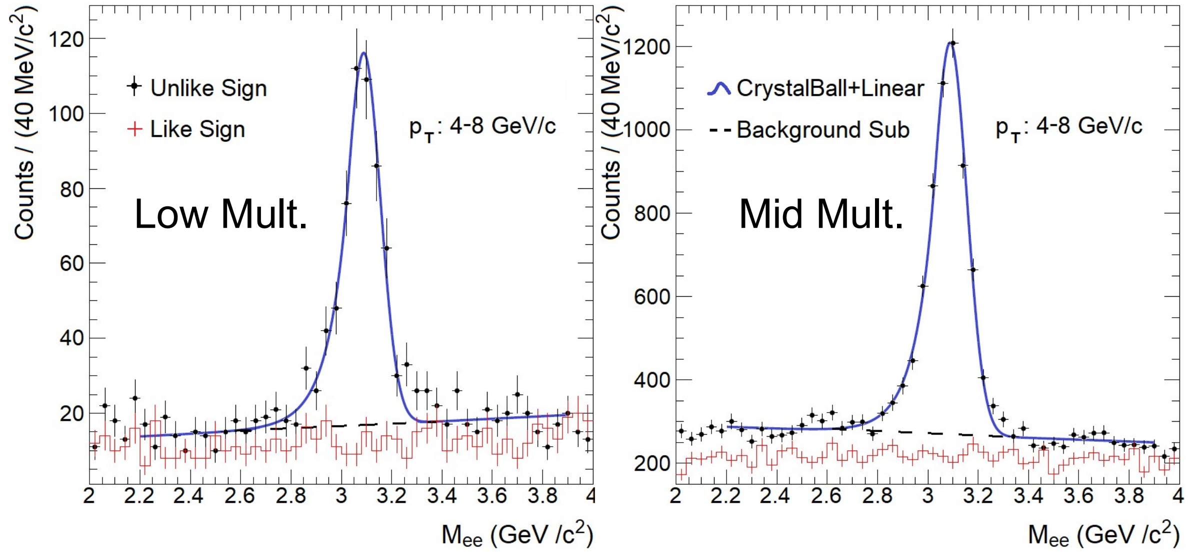

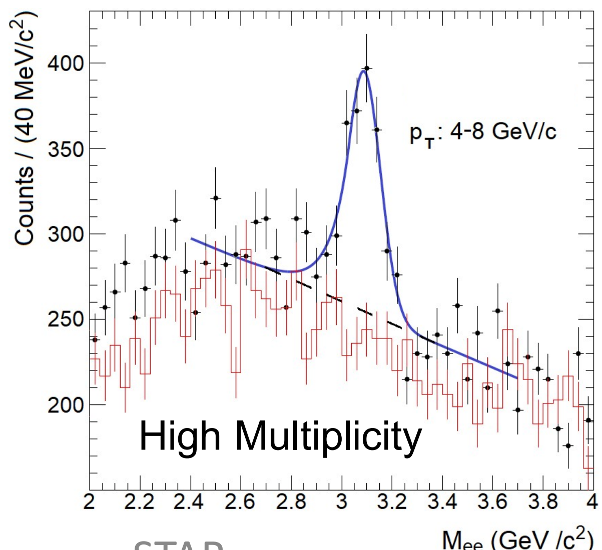

STAR

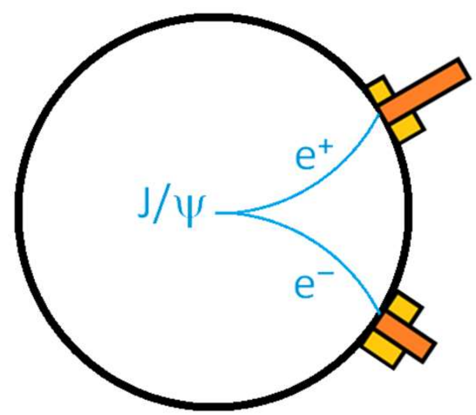

$$M^2 = (E_1 + E_2)^2 - \|\mathbf{p}_1 + \mathbf{p}_2\|^2$$

brennan.schaefer@lehigh.edu

Yield Extraction

- Yield extracted in
  $2.6 < M_{ee} < 3.4$ GeV/c^2
- Correct for yield beyond this region

- For systematic uncertainties do both function integration and histogram integration

- J/ψ yield normalized to the number of min-bias events

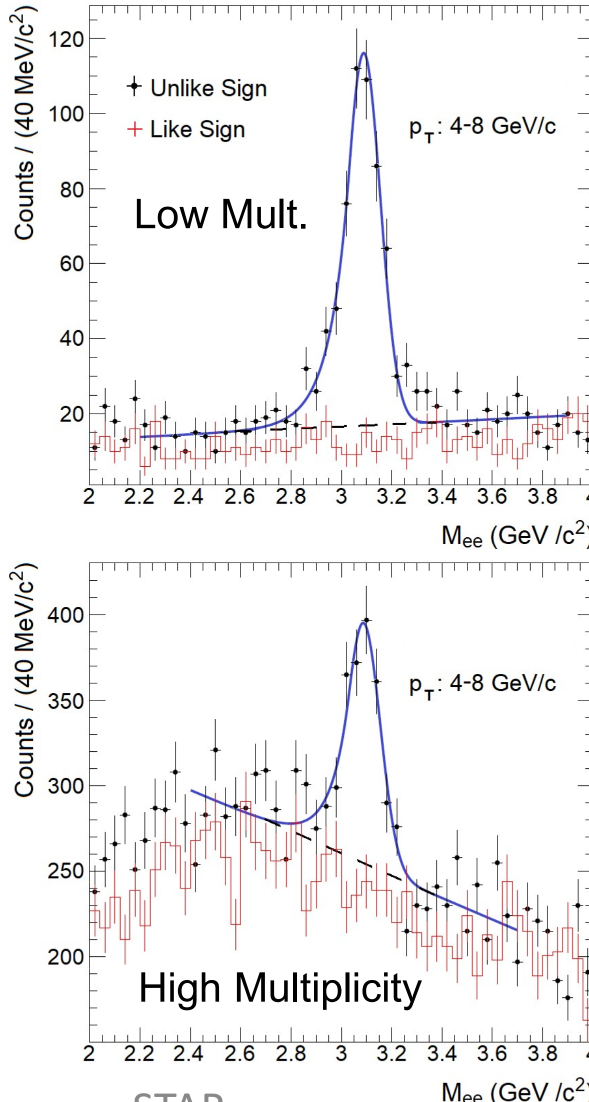
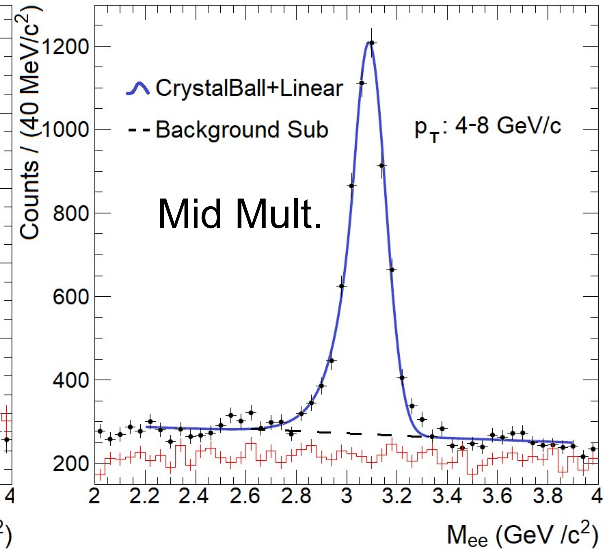

STAR

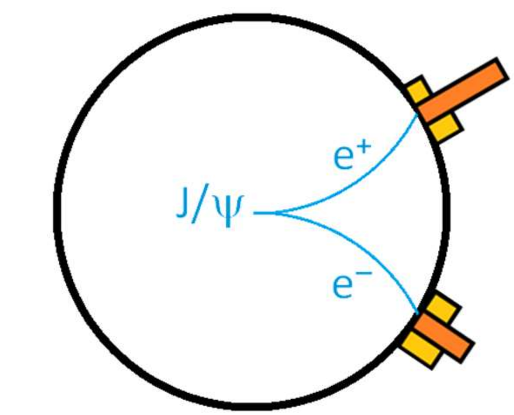

$$M^2 = (E_1 + E_2)^2 - \|\mathbf{p}_1 + \mathbf{p}_2\|^2$$

Uncertainties

Systematic Uncertainties				
	Track Quality			1 - 12%
	Daughter Electron Selection			1 - 9%
	Trigger Efficiency Correction			0 - 13%
	Signal & Background			3 - 16%
	Total			3 - 17%
Statistical Uncertainties				3 - 26%

Range of uncertainty variations:
different multiplicity intervals

Results

Higher reach in multiplicity than 200 GeV result

Improved multiplicity granularity

Normalized yields at 510 GeV consistent with 200 GeV

Hint of splitting between RHIC and LHC energies

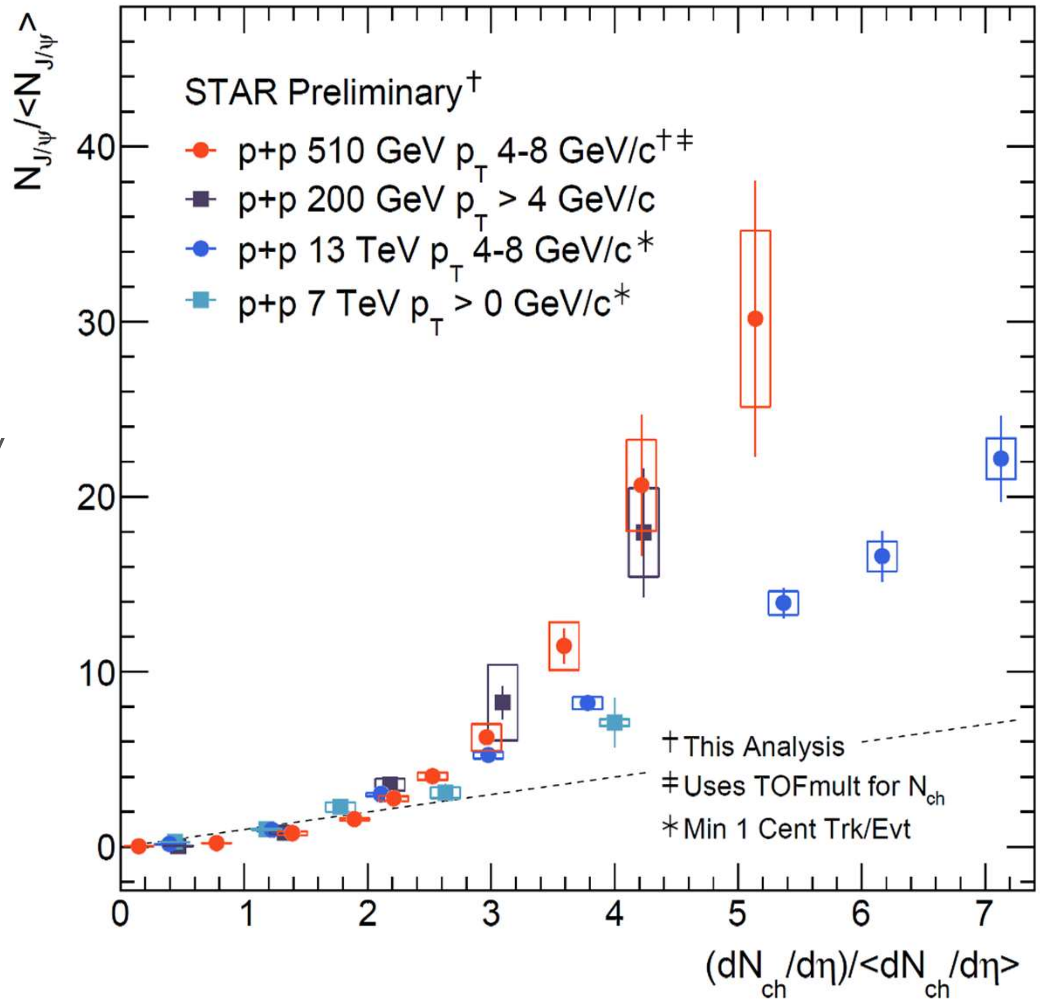

STAR, Physics Letters B 786 (2018) 87–93
ALICE, Phys. Lett. B 810 (2020) 135758
ALICE, Physics Letters B, 712 (2012) 165–175

Conclusion and Summary

- Unfolding is needed to convert TOF multiplicity into charged particle multiplicity
- Comparisons to different models and MC predictions
- Parallel study for Υ mesons in progress

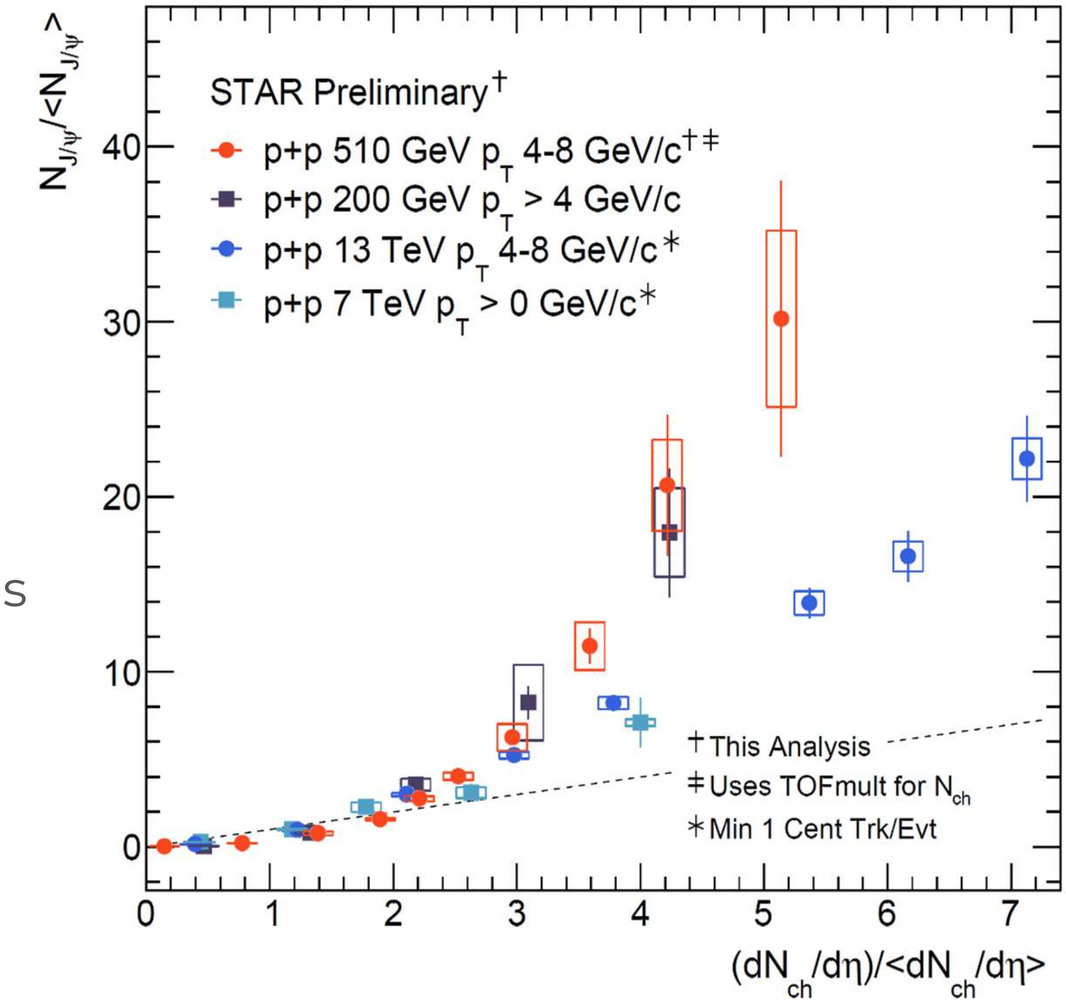

STAR, Physics Letters B 786 (2018) 87–93
ALICE, Phys. Lett. B 810 (2020) 135758
ALICE, Physics Letters B, 712 (2012) 165–175

Backup

References

[1] M. Kramer, Quarkonium Production at high-energy colliders, hep-ph/0106120

[2] J. Harris, B. Müller, et al, QGP Signatures revisited Eur. Phys. J. C (2024) 84:247

[3] J. Adam, J /ψ production cross section and its dependence on charged-particle multiplicity in p+p collisions at √s =200 GeV, Physics Letters B 786 (2018) 87–93

[4] Rubin P, et. al. (CLEO) Observation of the $^1P_1$ state of charmonium, Phys Rev D, 72 092004, 2005

[5] B. Abelev et. al. (ALICE) , J/ψ production as a function of charged particle multiplicity in pp collisions at √s = 7 TeV, Physics Letters B, 712 (2012) 165–175

[6] B. Martin, G. Shaw, Nuclear and Particle Physics, 3rd Ed, p. 190

[7] S. Acharya, et al. (ALICE) Multiplicity dependence of inclusive J/ψ production at √s = 13 TeV, Phys. Lett. B 810 (2020) 135758

[8] S. Weber, et al. Elucidating the multiplicity dependence of J/ψ production in proton-proton collisions with PYTHIA8, Eur. Phys. J. C (2019) 79:36

Backup

Model calculations at high multiplicity show qualitative agreement with measurements at LHC energy.

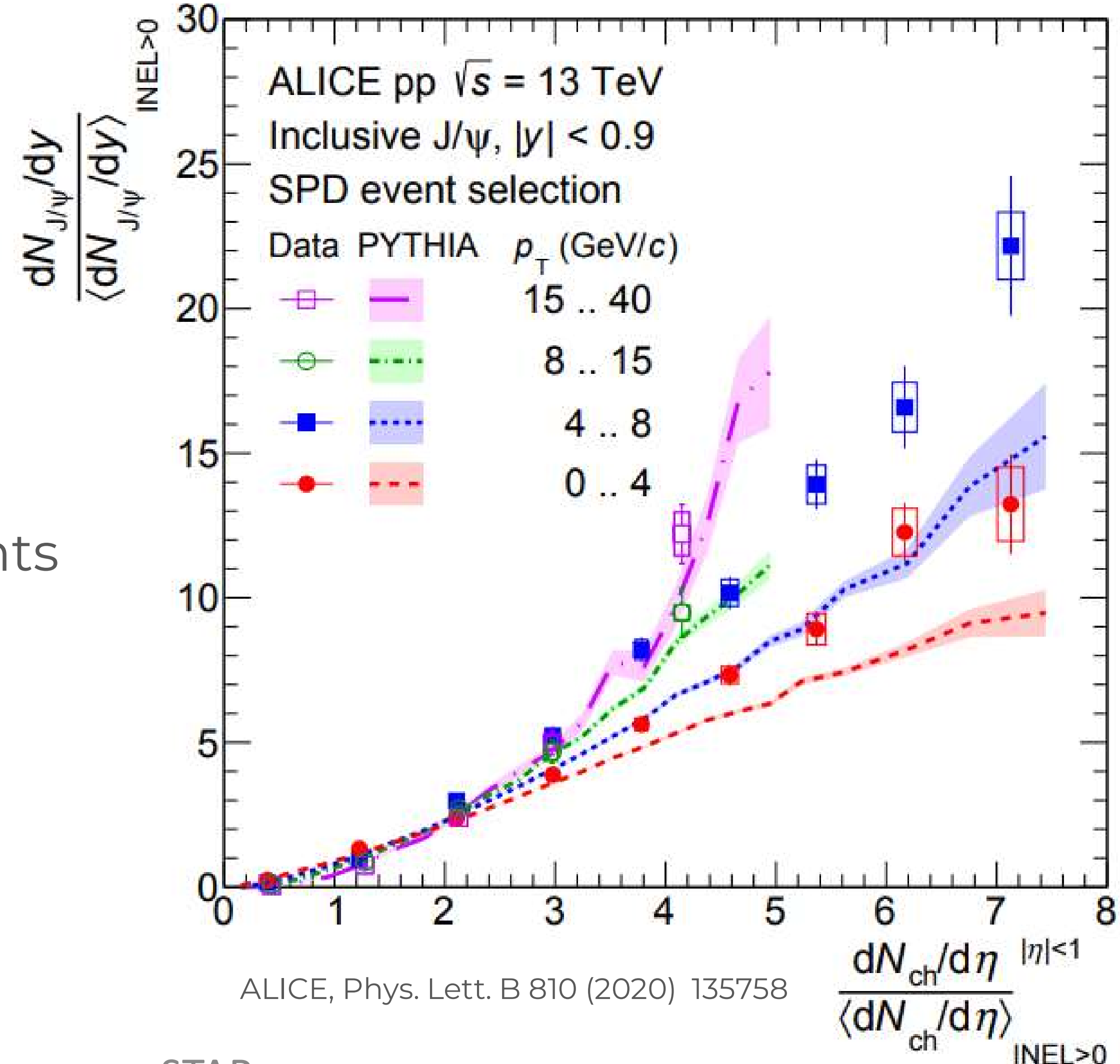

[7]

ALICE, Phys. Lett. B 810 (2020) 135758

Backup

Model calculations are able to describe the azimuthal distribution with respect to the J/ψ in underlying events

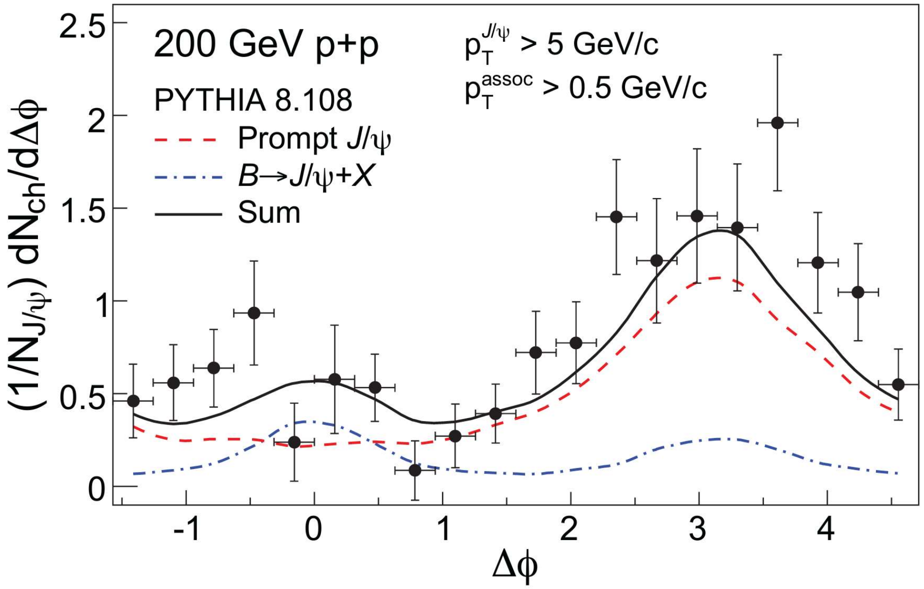

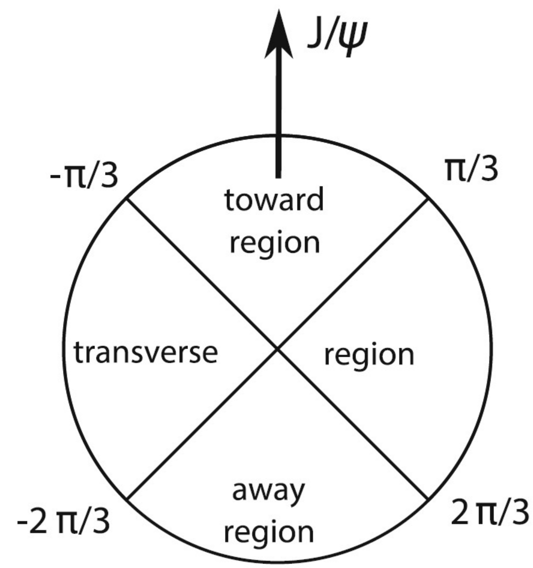

Backup

Comparable event activity dependence featured in production of other open and hidden heavy flavor hadrons

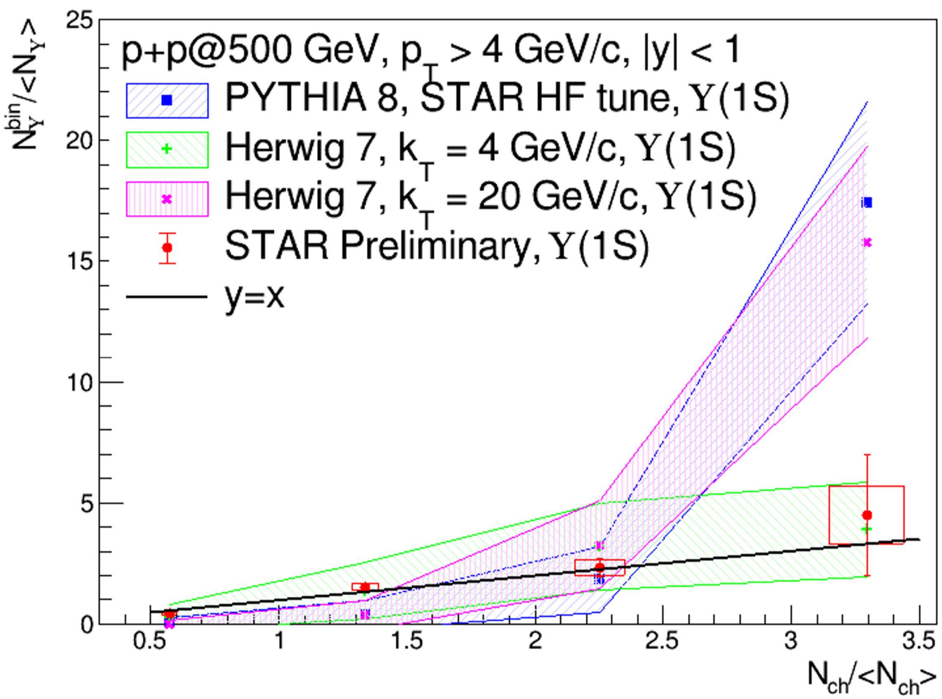

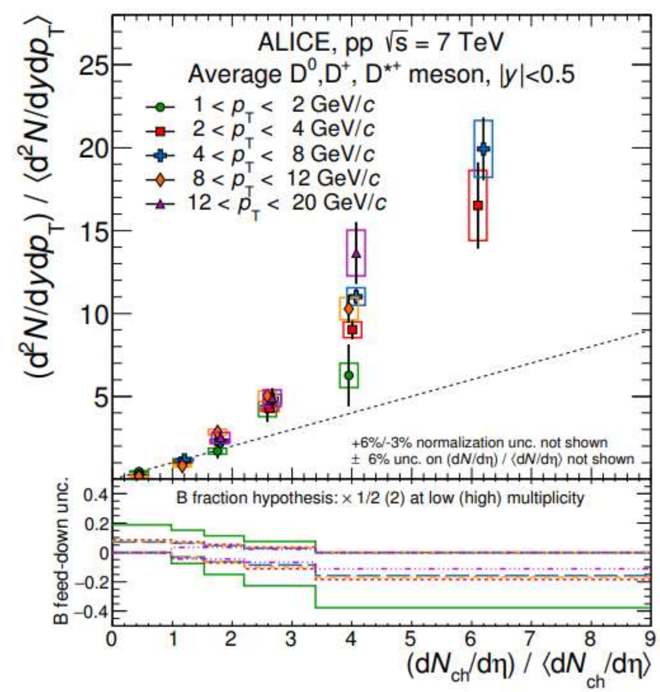

Backup

Separate efficiency vs multiplicity event selection corrections are necessary for the J/ψ and min-bias distributions

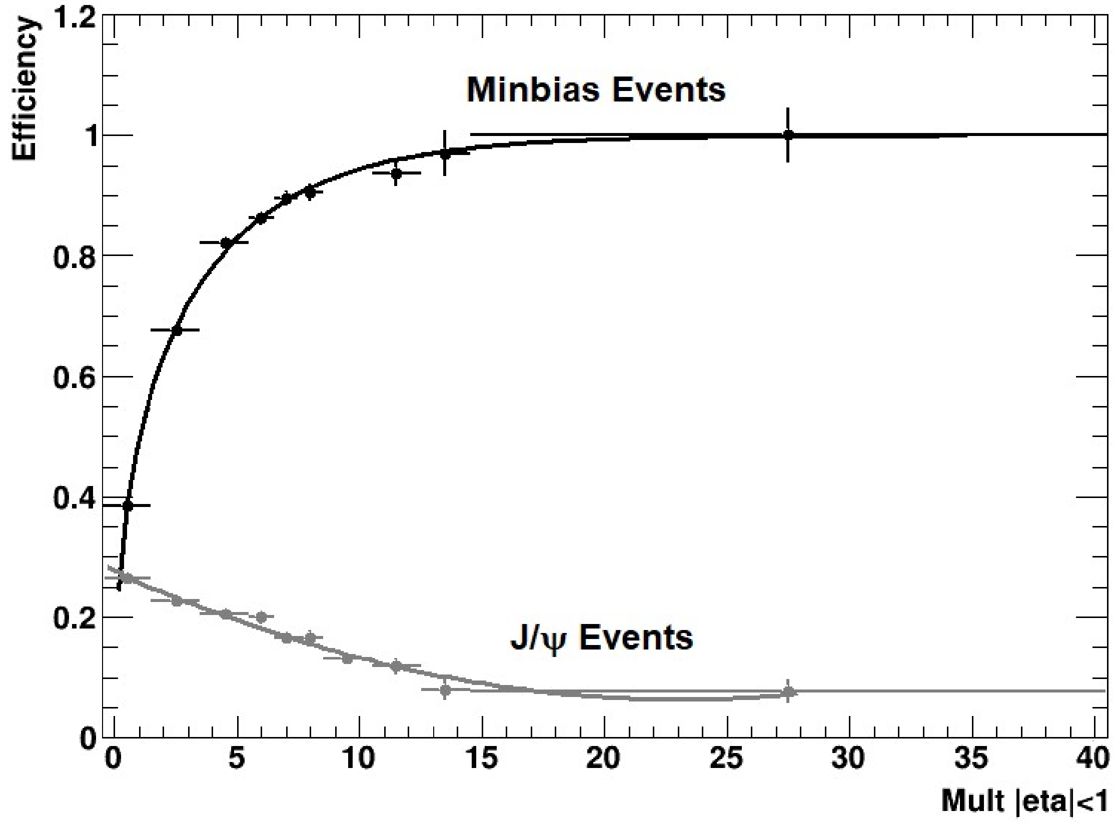

Pythia events

- STAR HF Tune
- MB

embedded into zerobias and reconstructed

Backup

$$F(Q^2) = \frac{G_E^2(Q^2) + \tau G_M^2(Q^2)}{1+\tau} + 2\tau \tan^2\left(\frac{\theta_e}{2}\right) G_M^2(Q^2)$$

- Within a **non-relativistic approach**, electromagnetic **form factors** can be interpreted as the **Fourier transform** of the charge and current **densities** inside the nucleon.

J.J. Kelly PRC 66 (2002) 065203

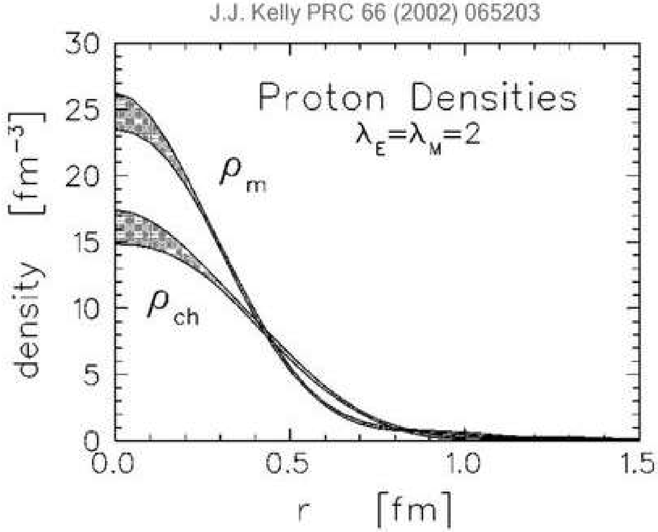

$$\rho_{ch}(r) = \frac{2}{\pi}\int_0^\infty dQ\, Q^2 j_0\left(Qr/\sqrt{1+\left(Q^2/4M^2\right)}\right) G_E\left(Q^2\right)\left[1+\left(Q^2/4M^2\right)\right]^{\lambda_E}$$

Dipole behaviour

$$\rho(r) = \frac{\lambda^3}{8\pi}\exp[-\lambda r] \rightarrow F(k) = \int \rho(r)\exp[ik\cdot r]d^3r = \frac{\lambda^4}{\left(k^2+\lambda^2\right)^2}$$

Backup

Further insight into this deviation from linearity can be obtained by investigating the impact parameter dependence of MPI. As mentioned earlier, in PYTHIA the number of MPI per event is related to the matter overlap in the pp collisions and, hence, to the impact parameter b [21]. Figure 3 (left panel) shows the average self-normalized number of MPI per event as a function of the self-normalized b^{-1}. In the most central collisions, the average number of MPI saturates at 3.3 times the mean value. Even higher number of MPI, as

[5]

5.2.1 The strong coupling constant

The strong interaction derives its name from the strong forces acting at distances of order 1 fm that, among other things, bind quarks in hadrons. However, many of the remarkable phenomena discussed in this chapter depend on the fact that the interaction gets weaker at short distances; that is, on asymptotic freedom. Such short-distance interactions are associated with large momentum transfers $|\mathbf{q}|$ between the particles, with

$$|\mathbf{q}| = \mathrm{O}(\hbar/r), \tag{5.6}$$

where $r = |\mathbf{r}|$ is the distance at which the interaction occurs. For example, the amplitude (1.47) for scattering from a spherically symmetric potential $V(r)$ becomes

$$\mathcal{M}(q) = 4\pi \int_0^\infty V(r) \left(\frac{\sin(qr)}{qr} \right) r^2 \mathrm{d}r \tag{5.7}$$

on integrating over all angular directions. The dominant contributions arise from r values of order q^{-1} as asserted, since for smaller r the integrand is suppressed by the factor r^2, while for large r it is suppressed by the average over the rapidly oscillating sine factor. Hence in discussing

[10] The numerical factor multiplying α_s (i.e. $-4/3$ in this case) depends on the colour state chosen, and we will not discuss it further.

[4]